

1 **Axenic amastigote cultivation and *in vitro* development of *Leishmania orientalis***

2

3 **Wetpisit Chanmol<sup>1</sup> • Narissara Jariyapan<sup>2</sup> • Pradya Somboon<sup>2</sup> • Michelle D. Bates<sup>3</sup> • Paul A. Bates<sup>3</sup>**

4

5 ✉ Narissara Jariyapan

6 njariyapan@gmail.com

7

8 <sup>1</sup>Graduate PhD's Degree Program in Parasitology, Faculty of Medicine, Chiang Mai University, Chiang Mai 50200,

9 Thailand

10 <sup>2</sup>Center of Insect Vector Study, Department of Parasitology, Faculty of Medicine, Chiang Mai University, Chiang Mai,

11 Thailand

12 <sup>3</sup>Division of Biomedical and Life Sciences, Faculty of Health and Medicine, Lancaster University, UK

13

14 **Abstract**

15 *Leishmania (Mundinia) orientalis* is a recently described new species that causes leishmaniasis in Thailand. To facilitate

16 characterization of this new species an *in vitro* culture system to generate *L. orientalis* axenic amastigotes was developed.

17 *In vitro* culture conditions of the axenic culture-derived amastigotes were optimized by manipulation of temperature and

18 pH. Four criteria were used to evaluate the resulting *L. orientalis* axenic amastigotes, i.e., morphology, zymographic

19 analysis of nucleases, cyclic transformation, and infectivity to the human monocytic cell line (THP-1) cells. Results

20 revealed that the best culture condition for *L. orientalis* axenic amastigotes was Grace's insect medium supplemented with

21 FCS 20%, 2% human urine, 1% BME vitamins, and 25 µg/ml gentamicin sulfate, pH 5.5 at 35 °C. For promastigotes, the

22 condition was M199 medium, 10% FCS supplemented with 2% human urine, 1% BME vitamins, and 25 µg/ml

23 gentamicin sulfate, pH 6.8 at 26 °C. Morphological characterization revealed six main stages of the parasites including

24 amastigotes, procyclic promastigotes, nectomonad promastigotes, leptomonad promastigotes, metacyclic promastigotes,

25 and paramastigotes. Also, changes in morphology during the cycle were accompanied by changes in zymographic profiles

26 of nucleases. The developmental cycle of *L. orientalis in vitro* was complete in 12 days using both culture systems. The

27 infectivity to THP-1 macrophages and intracellular growth of the axenic amastigotes was similar to that of THP-1 derived

28 intracellular amastigotes. These results confirmed the successful axenic cultivation of *L. orientalis* amastigotes. The

29 axenic amastigotes and promastigotes can be used for further study on infection in permissive vectors and animals.

30

31 **Keywords** *Leishmania* · Thailand · Axenic amastigote · Promastigote · Culture · Zymography

32

### 33 **Introduction**

34 At least 21 species of *Leishmania* parasites are known to cause leishmaniasis in humans. Infection results in three major  
35 types of disease: cutaneous leishmaniasis (CL); mucocutaneous leishmaniasis (MCL); and visceral leishmaniasis (VL),  
36 with about 0.9-1.3 million new cases and 20,000-30,000 deaths being reported annually (Akhoundi et al. 2017).  
37 *Leishmania* is a dioxenous parasite, with its life cycle comprising extracellular promastigote stages in an insect vector and  
38 intracellular amastigote stages in macrophages of a vertebrate host (Ghosh et al. 2003). Transmission from the insect  
39 vector to a mammalian host is achieved by inoculation of metacyclic promastigotes (Bates 2007). Promastigote stages  
40 can be relatively easily axenically cultivated in various types of media, whereas amastigote stages are more difficult to  
41 culture or obtain in large numbers free from host cell contaminants (Schuster and Sullivan 2002). However, the ability to  
42 culture amastigotes in axenic culture is extremely useful for studies on the biochemistry and molecular biology of the  
43 parasites, and for examining other aspects of their biology such as developmental cycle, infection, pathogenicity, and  
44 drug resistance.

45 Several methods and criteria have been used to characterize axenic amastigotes, comparing their properties to *in*  
46 *vivo* and/or *in vitro* promastigotes and/or intracellular amastigotes. For example, light microscopy (LM) and electron  
47 microscopy have been used to observe similarity in morphology (Hodgkinson et al. 1996). Changed status of lectin-  
48 mediated agglutination and membrane-bound enzymes, proteinase and nuclease activities, determination of total protein  
49 content, production of secretory acid phosphatase, and incorporation of thymidine, uridine and proline have all been used  
50 in analysis of biochemical properties (Bates 1994; Saar et al. 1998). In immunochemistry analyses, recognition by  
51 amastigote-specific monoclonal antibodies (mAbs) and differential expression of stage-specific antigens and cysteine  
52 proteinase-specific antigens have been reported. Genes encoding beta-tubulin and p100/11E or stage-specific genes such  
53 as Gp46, A2 and  $\beta$ -tubulin, have been used to characterize molecular properties (Rainey et al. 1991; Li et al. 2017).  
54 However, crucial criteria that should also be included in testing of axenic amastigote properties are cyclic transformation  
55 or expression of developmentally regulated gene(s) and infectivity or antigenic epitopes (Gupta et al. 2001). To date,  
56 axenic amastigotes that have been characterized extensively and are found to be essentially indistinguishable from  
57 genuine intracellular amastigotes include those of *Leishmania pifanoi*, *Leishmania mexicana*, and *Leishmania donovani*  
58 (Rainey et al. 1991; Bates et al. 1992; Debrabant et al. 2004).

59 Different culture conditions including temperature, pH and concentration of fetal calf serum (FCS) are required  
60 to be optimized for each species or strain (Teixeira et al. 2002). For example, *Leishmania braziliensis* and *Leishmania*  
61 *amazonensis* amastigotes required a relatively low pH (5.4) in the medium to transform, but not *Leishmania infantum*  
62 *chagasi*. Some reports describe the serial cultivation of *Leishmania* axenic amastigotes in cell-free medium with a  
63 complex composition, including a mixture of nucleotides and vitamins (Pan 1984), or with different protein sources and  
64 rabbit blood lysate (al-Bashir et al. 1992).

65 *Leishmania orientalis* is a new species that causes leishmaniasis among Thai patients (Jariyapan et al. 2018).  
66 The parasite is in the new subgenus *Mundinia*, previously called “*Leishmania siamensis*” (Espinosa et al. 2018). To  
67 facilitate characterization of this new species this study was undertaken in which first an *in vitro* culture system to generate  
68 *L. orientalis* axenic amastigotes was developed. *In vitro* culture conditions of the axenic culture-derived amastigotes were  
69 optimized by manipulation of temperature and pH. The resulting *L. orientalis* axenic amastigotes were evaluated by four  
70 criteria: (1) morphology, (2) zymographic analysis of nucleases, (3) cyclic transformation, and (4) infectivity to the human  
71 monocytic cell line (THP-1) cells, to confirm successful establishment of axenic amastigotes.

72

## 73 **Materials and methods**

### 74 **Parasite strain**

75 *L. orientalis* parasites (MHOM/TH/2014/LSCM4) were originally isolated from a skin lesion on the face of Thai woman  
76 patient (Jariyapan et al. 2018). The isolated parasites were initially grown as promastigotes in Schneider's insect medium  
77 (Sigma-Aldrich, St Louis, MO, USA), pH 6.8 supplemented with 20% (v/v) FCS (Life Technologies-Gibco, Grand  
78 Island, NY, USA) at 26 °C. Some were then cryopreserved as parasite culture stock at the Department of Parasitology,  
79 Faculty of Medicine, Chiang Mai University. As a routine promastigote culture, parasites were grown at 26 °C in M199  
80 medium, pH 6.8 with Hank's balance salt solution (HBSS) (Hyclone, Logan, UT, USA) supplemented with 10% (v/v)  
81 FCS, 2% (v/v) healthy human urine, 1% (v/v) Basal Medium Eagle (BME) vitamins (Sigma-Aldrich, St Louis, MO, USA)  
82 and 25 µg/ml gentamicin sulfate (Sigma-Aldrich, St Louis, MO, USA). Promastigotes were subpassaged to fresh medium  
83 every 4 days to maintain growth and viability of the parasites.

84

### 85 **THP-1 macrophage differentiation**

86 The human monocytic cell line (gift from Dr. Sirida Yangshim) was maintained in RPMI-1640 medium supplemented  
87 with 10% (v/v) FCS at pH 7.4 and 37 °C in a 5% CO<sub>2</sub> incubator. To maintain differentiation ability, the cells were  
88 subpassaged every 3 days to prevent cell density from exceeding 1 × 10<sup>6</sup> cells/ml. For cell differentiation, phorbol 12-  
89 myristate 13-acetate (PMA) was added into the THP-1 cell culture (2.5 × 10<sup>5</sup> cells/ml) on day 3 at a final concentration  
90 of 10 ng/ml (Jain et al. 2012). Following this, 200 µl of PMA-treated cells was dispensed to each well of 8-well Lab-Tek  
91 culture chamber slides. The cells were incubated at 37 °C, 5% CO<sub>2</sub> for 48 h to allow complete differentiation of the cells.  
92 After the 48 h incubation period, the cells were washed with pre-warmed culture medium and then used for infection  
93 assays.

94

### 95 **Generation of THP-1-derived intracellular amastigotes**

96 To generate THP-1-derived intracellular amastigotes, promastigotes in the stationary growth phase were used to infect  
97 THP-1 macrophages at a ratio of 10:1 parasites/cell. Cells were then incubated in tissue culture flasks at 35 °C, 5% CO<sub>2</sub>.  
98 After incubation for 8 h, the non-internalized promastigotes were removed by washing three times with pre-warmed  
99 RPMI-1640 medium and incubated in the same medium supplemented with 10% FCS for an additional 72 h. The cells  
100 were then washed with serum-free RPMI-1640 medium and removed from the culture plate by using a cell scraper. The  
101 cells were then washed and suspended in the serum-free RPMI-1640 medium, and passaged 10 times through a sterile  
102 26-gauge needle. The homogenized suspension was centrifuged for 3 min at 300×g. The resulting supernatant was  
103 recovered and centrifuged at 1,000×g for 5 min to collect the amastigotes. The pellet of amastigotes (~ 5 × 10<sup>6</sup> cells) was  
104 resuspended in the RPMI-1640 medium supplemented with 10% FCS and 25 µg/ml of gentamicin sulfate for subsequent  
105 experiments.

106

107 **Ficoll density gradient centrifugation for enrichment of *L. orientalis* nectomonad promastigotes, leptomonad**  
108 **promastigotes, and metacyclic promastigotes**

109 Ficoll density gradient centrifugation for enrichment of *L. orientalis* nectomonad promastigotes, leptomonad  
110 promastigotes, and metacyclic promastigotes was adapted from methods described by Späth and Beverley (2001) and  
111 Yao et al. (2008) as shown in Fig. 1. Stages of *L. orientalis* parasites were assigned according to the classification  
112 described by Rogers et al. (2002). To prepare a 10%-20%-40% discontinuous Ficoll density gradient, a 40% stock solution  
113 of Ficoll Type 400 (Sigma, UK) was prepared in phosphate buffered saline (PBS), stored at 4 °C and used within a month.  
114 Twenty percent of Ficoll in Schneider's insect medium without serum and 10% Ficoll in M199 medium without serum  
115 were prepared on the day that they were used by diluting from the stock solution. The working solutions were then filtered  
116 through a 0.22 µm cellulose acetate filter, separately. The 10-20-40% discontinuous Ficoll density gradient was prepared  
117 in a 15 ml conical tube by carefully loading 2 ml of 40% Ficoll-PBS at the bottom, then 2 ml of 20% Ficoll- Schneider's  
118 insect medium in the middle, and 2 ml of 10% Ficoll-M199 medium on the top. The Ficoll density gradient was used  
119 immediately to maximize the homogeneity of nectomonad promastigotes, leptomonad promastigotes, or metacyclic  
120 promastigotes. Samples of each promastigote form were collected as follows. Initially, THP-1-derived intracellular  
121 amastigotes were cultured in M199 medium, 10% FCS supplemented with 2% human urine, 1% BME vitamins, and 25  
122 µg/ml gentamicin sulfate, pH 6.8 at 26 °C. A culture with a high proportion of nectomonad promastigotes was collected  
123 on day 3 (passage [P] 0). To produce higher numbers of leptomonad promastigotes and metacyclic promastigotes the  
124 promastigote culture (P0) at day 3 was subpassaged into fresh medium and incubated for further 5 days to collect culture  
125 with a high proportion of leptomonad promastigotes (P1) and 7 days for a high proportion of metacyclic promastigotes  
126 (P1). Each sample of culture parasites was pelleted at 2,000×g for 10 min at room temperature. Each pellet sample was  
127 resuspended in 2 ml Schneider's insect medium to adjust parasite density to 2 × 10<sup>8</sup> cells/ml and gently applied to the top

128 of the Ficoll density gradient. The gradient was then centrifuged for 15 min at 400×g at room temperature. Nectomonad  
129 promastigote-enriched and leptomonad promastigote-enriched populations were recovered between 10 and 20%  
130 discontinuous gradients, and a metacyclic promastigote-enriched population was found between 0 and 10% discontinuous  
131 gradients of the Ficoll interfaces. Each enriched population was carefully collected, transferred into a 1.5 ml sterile  
132 microcentrifuge tube, and centrifuged at 2,000×g for 10 min at room temperature. The supernatant was discarded and the  
133 pellet was stored at -20 °C until used. The percentage of the promastigote-enriched population of each form was quantified  
134 by staining with 5% Giemsa's solution and counted under a light microscope.

135

### 136 **Optimization of amastigote culture conditions and growth kinetics of *L. orientalis* axenic amastigotes**

137 The culture conditions for generating axenic amastigotes were optimized by varying parameters including temperature  
138 and pH. In these experiments, Grace's insect medium was used to investigate the optimum temperature for transformation  
139 of promastigotes to amastigotes. Promastigotes ( $2 \times 10^6$  cells/ml) at the stationary phase were used as initial cells. They  
140 were subpassaged into 5 ml of the tested media at pH 5.5 and incubated at 32, 34 or 36 °C for 96 h. All media used in this  
141 study were supplemented with FCS 20% (v/v), 2% (v/v) human urine, 1% (v/v) BME vitamins, and 25 µg/ml gentamicin  
142 sulfate. After 96 h incubation, all cultures were examined for amastigote-like forms under an inverted microscope  
143 (Olympus, Tokyo, Japan). After obtaining the temperature that facilitated promastigote transformation to amastigote  
144 forms, experiments to optimize pH were performed. Acidity of the culture media was adjusted from acidic to neutral pH  
145 levels, at pH 5.5, 6.0, 6.5 and 7.0. All experimental cultures were incubated at the optimum temperature for 5 days. Small  
146 aliquots of each culture were collected daily and parasite counts were performed using a hemocytometer (Precicolor HBG,  
147 Germany) for the percentage of parasite forms (% parasite forms) and parasite density. Morphological criteria used to  
148 identify a typical amastigote form in the culture included an ovoid body form with no flagellum protruding from the  
149 flagellar pocket (Rogers et al. 2002). A trypan blue dye exclusion test (Fluka, Buchs, Switzerland) was used to evaluate  
150 cell viability.

151

### 152 **SDS-PAGE zymography of nucleases**

153 SDS-PAGE zymography described by Joshi et al. (2012) with some modifications was used to analyze nuclease activity  
154 against polyadenylic acid (poly (A)) of *L. orientalis* THP-1-derived intracellular amastigotes, promastigote forms, and  
155 axenic amastigotes. Cell lysate ( $\sim 5 \times 10^6$  cells) of each sample was lysed in a lysis buffer containing 1% SDS, 25 mM  
156 Tris/192 mM glycine pH 8.5, 50 µg/ml leupeptin, mixed with a non-reducing buffer for SDS-PAGE and boiled for 5 min.  
157 The prepared sample was loaded in each well and separated on 12.5% (w/v) SDS polyacrylamide gels containing poly  
158 (A) as a substrate under non-reducing conditions at the final concentration of 0.3 mg/ml. Electrophoresis was carried out  
159 under constant voltage (120 V) at 25 °C for 2 h 30 min. After the separation, gels were washed at room temperature with

160 renaturation buffer (100 mM HEPES, 0.1% (v/v) Triton X-100, pH 8.5) for four times and then incubated in the same  
161 buffer for 45 min at 37 °C. Subsequently, gels were rinsed and fixed with 7.5% (v/v) acetic acid aqueous solution before  
162 staining with Toluidine Blue O and de-staining with deionized water. Activity of nucleases against poly (A) was visible  
163 as clear bands within a blue staining gel.

164

#### 165 **Developmental cycle of *L. orientalis* in vitro**

166 To investigate the developmental cycle of *L. orientalis* in vitro, initially, axenic amastigotes ( $1 \times 10^6$  cells/ml) were  
167 cultured in M199 medium supplemented with 10% (v/v) FCS, 2% (v/v) human urine, 1% (v/v) BME vitamins, and 25  
168  $\mu\text{g/ml}$  gentamicin sulfate, pH 6.8 at 26 °C. When the parasite population was largely composed of metacyclic  
169 promastigotes, the parasites ( $1 \times 10^6$  cells/ml) were then transferred to the optimal culture medium for axenic amastigotes.  
170 During cultivation, aliquots to prepare cell lysates of each culture were harvested daily by centrifugation of parasites at  
171  $2,000\times g$  for 10 min, and washed three times with PBS. The collected samples were used for SDS-PAGE zymography for  
172 nucleases as described here. Also, cell density was recorded daily throughout the period of cultivation. Experiments were  
173 performed in triplicate.

174

#### 175 **Light microscopy**

176 The morphological characteristics of the parasites including cell body length and width, flagellum length, and nuclear-  
177 kinetoplast position were measured and analyzed using an Olympus CX31 light microscope (Olympus America Inc.,  
178 USA) at  $\times 1,000$  magnification. Five microliters of culture collected from the axenic culture were smeared on microscopic  
179 slides. The slides were air-dried, fixed in methanol and stained with 5% (v/v) Giemsa's stain solution. Morphological  
180 forms based on previous descriptions by Rogers et al. (2002) were used to classify the parasites into categories. A  
181 minimum of 200 parasites were examined and classified at each time point.

182

#### 183 **SEM and TEM**

184 For SEM, parasites were collected from the exponential phase of the culture. Parasites were allowed to settle on poly-L-  
185 lysine coated glass coverslips and fixed with 2.5% glutaraldehyde in 0.1 cacodylate buffer (pH 7.2) for 1 h at 4 °C. After  
186 washing with the same buffer, the cells were dehydrated in a graded series of ethanol (50%, 70%, 90%, 95% for 10 min  
187 each and then twice with 100% ethanol for 30 min each), followed by critical point drying in liquid  $\text{CO}_2$  and coated with  
188 gold particles. The gold-coated preparations were examined under a scanning electron microscope, JEOL JSM-5910  
189 (JEOL, Tokyo, Japan), at 25-30 kV.

190 For TEM, the harvested culture parasites were pelleted and washed twice with PBS pH 7.2. The samples were  
191 fixed in 2.5% glutaraldehyde and 5 mM  $\text{CaCl}_2$  in 0.1 M cacodylate buffer pH 7.2 for 1 h or overnight at 4 °C and then

192 washed in the same buffer and post fixed in 1% osmium tetroxide, 0.8% potassium ferrocyanide and 5 mM CaCl<sub>2</sub> in 0.1  
193 M cacodylate buffer pH 7.2. The samples were then washed with 0.1 M cacodylate buffer pH 7.2 and subsequently  
194 dehydrated in a graded acetone series (50%, 70%, 90%, 95% for 10 min each and then twice with 100% acetone for 30  
195 min each). Finally, the samples were embedded in a mixture of Araldite-Epon. Ultra-thin sections were cut using Leica  
196 Ultramicrotome UCT (Leica, Austria). Sections were stained with lead citrate and 1% uranyl acetate. The stained sections  
197 were examined under a transmission electron microscope, JEOL JEM-2200 FS (JEOL, Tokyo, Japan), at 80 kV.

198

### 199 **Comparison of infectivity in THP-1 cells between THP-1-derived intracellular amastigotes and axenic amastigotes**

200 THP-1 macrophages were grown in eight-chamber Lab-Tek tissue culture slides and infected at a 5:1 parasite to  
201 macrophage ratio with either the THP-1-derived intracellular amastigotes or the axenic amastigotes for 8 h at 35 °C in  
202 5% CO<sub>2</sub>. Subsequently, these cultures were washed three times with pre-warmed RPMI-1640 medium to remove non-  
203 internalized parasites. The chamber slides containing the infected macrophages were incubated at 35 °C, 5% CO<sub>2</sub>. Then  
204 slides were incubated for an additional 16, 40 or 64 h, fixed, stained with 5% (v/v) Giemsa's stain solution and processed  
205 for light microscopy (Debrabant et al. 2004). Experiments were performed in triplicate. A minimum of 200 macrophages  
206 was counted from each chamber. Results of these experiments were expressed as the percentage of infected macrophages,  
207 the average number of amastigotes per macrophage, and the infection index. The infection index was determined by  
208 multiplying the percentage of infected macrophages by the average number of amastigotes per macrophage (Paladi et al.  
209 2012).

210

### 211 ***In vitro* intracellular amastigote growth**

212 Evaluation of amastigote replication was performed at 8, 24, 48, and 72 h post infection by light microscopic  
213 determination of average infection index of 200 Giemsa-stained macrophages. Experiments were performed in triplicate.  
214 To allow comparison, the infectivity at 8 h post-infection was used as an internal baseline control (T0). Amastigote  
215 multiplication ratio was calculated using the following formula:

$$216 \text{ Amastigote multiplication ratio} = \frac{\text{no. of amastigotes at Tx}}{\text{no. of amastigote at T0}}$$

217

### 218 **Statistical analysis**

219 All statistical analyses were performed using GraphPad Prism version 6.0 software. Statistical differences between  
220 intracellular and axenic amastigotes were determined using two-way ANOVA with Bonferroni's *post hoc* multiple  
221 comparisons for infection index and intracellular multiplication ratio. Tests were considered statistically significant if *P*  
222 < 0.05.

223

## 224 **Results**

### 225 **Zymographic analysis of nucleases of THP-1-derived intracellular amastigotes and promastigote forms of *L.*** 226 ***orientalis***

227 To search for markers to differentiate between amastigotes and promastigote forms, SDS-PAGE zymography of nucleases  
228 was used to analyze nuclease profiles of pure *L. orientalis* intracellular amastigotes harvested from infected THP-1  
229 macrophages (100% purity), procyclic promastigotes collected on day 2 (~ 89% purity), nectomonad promastigote-  
230 enriched population (~ 85% purity), leptomonad promastigote-enriched population (~ 88% purity), and metacyclic  
231 promastigote-enriched population (~ 84% purity) (Table 1). The nuclease profile of the THP-1-derived intracellular  
232 amastigotes was detected on the gel with molecular masses of 27, 29, and 32 kDa while the promastigote forms processed  
233 nuclease bands with molecular masses of 27, 29, 30, and 32 kDa with different intensities except for the metacyclic  
234 promastigote-enriched population in which no 29 kDa band was observed (Fig. 2). Therefore, the differences of the  
235 zymographic profiles of nucleases between the intracellular amastigotes and promastigote forms were used as markers to  
236 identify *in vitro* axenic amastigotes in further experiments.

237

### 238 **Optimization of conditions for *L. orientalis* axenic amastigote cultivation**

239 To generate axenic amastigotes of *L. orientalis*, optimizations of temperature and pH for cultivation were performed.  
240 Initially, to optimize temperature that allows promastigotes to transform to amastigotes, Grace's insect medium  
241 supplemented with FCS 20% (v/v), 2% (v/v) human urine, 1% (v/v) BME vitamins, and 25 µg/ml gentamicin sulfate and  
242 adjusted pH to 5.5 was used and temperature was varied at 32, 34 and 36 °C. Results showed that after incubation for 96  
243 h at 32 °C, all parasites were in promastigote forms (still in possession of an external flagellum). No amastigote-like form  
244 was found. At 34 °C some amastigote-like forms, characterized by an ovoid body form with no flagellum protruding from  
245 the flagellar pocket, were observed using LM (Fig. 3a). Ultrastructural morphology of the axenic amastigotes was  
246 revealed by TEM (Fig. 3b). General features of *L. orientalis* amastigotes included an ovoid shape with a body width of  
247 2-4 µm, a short non-emergent flagellum, and the absence of a paraflagellar rod. At 36 °C most parasites died.

248 The acidity of culture media was also varied by adjusting the pH of the culture medium from acidic to neutral  
249 levels at pH 5.5, 6.0, 6.5 and 7.0. Promastigote transformation into amastigotes occurred within 24 h in all tested pH at  
250 34 °C. However, it was only in the media with pH 5.5 and 6.0 that all promastigotes had completely transformed into  
251 amastigotes on day 5 of cultivation with final cell density  $22.72 \times 10^6$  and  $21.76 \times 10^6$  cells/ml, respectively. At 34 °C,  
252 pH 5.5 on day 5, cell viability evaluated by trypan blue dye began to fall (lower than 95%), unless cultures were  
253 supplemented with fresh medium. When the cultured amastigotes from these conditions were subcultured in fresh culture  
254 medium, pH 5.5 and incubated at 34 °C, a low growth rate was obtained (a mean doubling time =  $153.9 \pm 19.57$  h) with



255 approximately 98% of viable cells. However, when the duplicated cultured amastigotes were incubated at 35 °C, the  
256 growth rate of the parasites increased with a mean doubling time of  $22.76 \pm 0.07$  h. Therefore, the axenic amastigotes  
257 were subpassaged every 4 days in fresh Grace's insect medium, supplemented with FCS 20% (v/v), 2% (v/v) human  
258 urine, 1% (v/v) BME vitamins, and 25 µg/ml of gentamicin sulfate, pH 5.5 and incubated at 35 °C. Under these culture  
259 conditions, it was possible to maintain amastigote cultures continuously for a period of at least 3 months, involving more  
260 than 22 subpassages.

261

### 262 **Zymographic analysis of nucleases of *L. orientalis* axenic amastigotes**

263 The zymographic profiles of nucleases of the axenic amastigotes (P0, P1, P5, P10, and P20) (Fig. 4) were similar to that  
264 of the intracellular amastigotes derived from infected THP-1 macrophages but different from *in vitro* promastigotes (as  
265 shown in Fig. 2).

266

### 267 **Cyclic transformation and development of *L. orientalis* in axenic culture**

268 To investigate cyclic transformation and generate a complete life cycle of *L. orientalis in vitro*, two culture systems for  
269 cultivation of amastigotes and promastigotes were combined. Axenic amastigotes ( $1 \times 10^6$ /ml) were used as initial cells  
270 and cultured in M199 medium supplemented with 10% (v/v) FCS at pH 6.8, and incubated at 26 °C. Under these  
271 conditions the amastigotes transformed to promastigote forms within 24 h. During days 1-7 of cultivation, various  
272 promastigote forms were observed and identified. These included procyclic promastigotes, nectomonad promastigotes,  
273 leptomonad promastigotes, metacyclic promastigotes and paramastigotes. Morphological categories and the fine structure  
274 of six developmental forms of *L. orientalis* in the axenic culture are shown in Table 2 and Fig. 5. Morphometric data  
275 including body length, width, flagellum length and nucleus-kinetoplast position of the parasites at each developmental  
276 stage are shown in Table 3.

277 The relative percentages of amastigotes and several developmental forms of promastigotes were determined  
278 from Giemsa-stained smears (Fig. 6a). Procyclic promastigotes were observed at the highest proportion on day 1 after  
279 subculturing (~ 78%). The procyclic population was higher than other forms on days 1-4 (~ 70%) and decreased after day  
280 5 until its proportion was near zero on day 7. Nectomonad promastigotes were observed from days 2-7 with a proportion  
281 of ~ 20% on day 2 and the highest population on day 3 (~ 25%) and then the proportion had decreased to ~ 10% on day  
282 7. Leptomonad promastigotes were found on days 3-7 but dominated on days 5-7 with the proportion of ~ 40-50%.  
283 Metacyclic promastigotes were observed from day 5 and increased continuously until day 7. Paramastigotes were  
284 observed from day 6 but the peak of population was found on day 7 (~ 27%). When the promastigotes were left in the  
285 same culture for 10 days the paramastigote population started to decrease to ~ 10% and ~ 3% on day 8 and day 10,  
286 respectively. At the stationary phase on day 7, the highest population of metacyclic promastigote forms (~ 20%) was

287 obtained (Fig. 6a). Then, these parasites ( $1 \times 10^6$ /ml) were subcultured into Grace's insect medium supplemented with  
288 FCS 20% (v/v), 2% (v/v) human urine, 1% (v/v) BME vitamins, and 25  $\mu$ g/ml gentamicin sulfate, pH 5.5 and incubated  
289 at 35°C (the optimal medium and condition for axenic amastigotes). The metacyclic promastigotes resorbed their flagella  
290 and adopted a rounded morphology within 24 h. On day 8, ~ 15 % of the rounded aflagellate population and ~ 85% of an  
291 intermediate form population (round body cells with a flagellum shorter than body length or a short stump) were observed.  
292 The amastigote-like forms subsequently propagated in the axenic culture. Amastigote-like forms accounted for 100% of  
293 the parasite population were observed on day 12 onwards (Fig. 6a). Parasite density in the cultures from days 1-12 is  
294 shown in Fig. 6b.

295 Nuclease zymographic profiles were used to assist in defining life cycle forms of *L. orientalis*. Therefore,  
296 changes in the zymographic profiles of the parasites harvested daily during their developmental cycle in the *in vitro*  
297 cultures were analyzed. The axenic amastigotes (day 0) possessed three prominent bands of the apparent molecular masses  
298 27, 29 and 32 kDa. Upon transformation to promastigotes, the intensity of the bands was decreased from days 1-6 and on  
299 day 7, the 29 kDa band was undetectable. In addition, from days 4-7 an additional band with a molecular mass of 30 kDa  
300 was observed when the promastigote population was predominant. After transferring the promastigotes to the Grace's  
301 insect medium under the optimum condition for amastigote culture, the 30 kDa band completely disappeared on day 8.  
302 Also, a marked increase in intensity of the 27, 29 and 32 kDa bands was noted, thus the nuclease profile of the amastigotes  
303 was restored from days 8-12 (Fig. 7).

304

### 305 **Comparison of infectivity in THP-1 cells and intracellular growth between axenic amastigotes and THP-1-derived** 306 **intracellular amastigotes**

307 Infectivity of the axenic amastigotes and the THP-1-derived intracellular amastigotes in THP-1 cells was determined and  
308 compared (Fig. 8a). The infection index of axenic amastigotes was relatively higher than that of the intracellular  
309 amastigotes during the first 48 h of infection. However, at the 72 h after infection, the infection indices of both axenic  
310 amastigotes and intracellular amastigotes were not statistically different and the average number of parasites per cell was  
311 similar (approximately four parasites/cell). An increase in the amastigote multiplication ratio was observed at all time  
312 points in both axenic and THP-1 derived amastigotes but no statistical difference in the ratios was found (Fig. 8b).

313

### 314 **Discussion**

315 In this study, the axenic cultivation of *L. orientalis* amastigotes was successfully established for the first time, which has  
316 also not been previously reported for any other member of the new subgenus *Mundinia*. This *in vitro* culture system was  
317 devised to mimic some of the environmental conditions that intracellular amastigotes would encounter within the  
318 phagolysosomal system of macrophages of vertebrate hosts including temperature and acidic pH. Since *L. orientalis*

319 causes CL (Jariyapan et al. 2018), the optimum temperature obtained in this study for growing axenic amastigotes was  
320 relevant to its clinical manifestation. *L. orientalis* amastigote-like forms were observed after incubation for 96 h at 34 °C  
321 but all promastigotes completed their transformation to amastigotes at 35 °C. Not only the temperature but also the acidity  
322 of the culture medium is an essential factor for transformation and retention of the amastigote morphology. *L. orientalis*  
323 was able to retain the morphology as amastigotes at pH 5.5. These finding were similar to that demonstrated in other  
324 species of *Leishmania* (Debrabant et al. 2004). This adaptation may partly account for the ability of amastigotes to survive  
325 and multiply within the acidic environment of the phagolysosomes *in vivo*. Several physiological activities of amastigotes  
326 such as respiration, catabolism of energy substrates and incorporation of precursors into macromolecules are carried out  
327 optimally at pH 4.5-5.5, whereas these activities are optimal at or near neutral pH for promastigotes (Moradin and  
328 Descoteaux 2012). Therefore, the optimum condition for generation of *L. orientalis* axenic amastigotes in this study was  
329 using Grace's insect medium, supplemented with FCS 20% (v/v), 2% (v/v) human urine, 1% (v/v) BME vitamins, and  
330 25 µg/ml of gentamicin sulfate, pH 5.5, incubated at 35 °C. As revealed by LM and TEM *L. orientalis* axenic amastigotes  
331 processed general morphological features (ovoid in shape, 2-4 µm on the body width, a short non-emergent flagellum,  
332 and no paraflagellar rod) similar to that reported for other *Leishmania* species (Gupta et al. 2001; Sunter and Gull 2017).

333 *Leishmania* species that cause the same or different form of disease may require specific culture conditions, for  
334 example, *L. mexicana*, a causative agent of CL, amastigotes can be cultivated axenically under conditions of 32 °C, pH  
335 5.5 (Bates 1994). In *Leishmania* species that cause VL, for example, *L. donovani* and *Leishmania tropica*, these species  
336 required incubation at 37 °C, pH 5.5 with CO<sub>2</sub> to transform into axenic amastigote-like form (Debrabant et al. 2004). In  
337 the case of *L. amazonensis*, a species associated with cutaneous and diffuse cutaneous leishmaniasis, extracellular  
338 amastigote-like form can be maintained in axenic culture at 32 °C, pH 4.6. It grows in continuous culture at a lower  
339 temperature and pH than any other species characterized to date (Hodgkinson et al. 1996).

340 Analysis of the nuclease profile of *L. orientalis* axenic amastigotes at subpassages P0, P1, P5, P10, and P20 by  
341 SDS-PAGE zymography revealed that for survival and development the axenic amastigotes processed only three nuclease  
342 bands at molecular masses of 27, 29, and 32 kDa with high intensity in all subpassages as found in the THP-1-derived  
343 intracellular amastigotes. Procyclic promastigotes, nectomonad promastigotes, and leptomonad promastigotes expressed  
344 the nuclease activity at molecular masses of 27, 29, 30, and 32 kDa apart from metacyclic promastigotes in which the 29  
345 kDa band was undetectable. These results indicate that the 30 kDa nuclease was specific in all promastigote forms and  
346 might be important for their development. In the case of the 29 kDa nuclease, it might be unnecessary for metacyclic  
347 promastigotes in their development and/or other functions, for example, infection. Identification and characterization of  
348 these enzymes in their type, kinetics and other properties should be performed to investigate their roles in each parasite  
349 forms and compare to other *Leishmania* species.

350 One of the important criteria used to characterize axenic amastigotes is ability of the axenic amastigotes to

351 differentiate back to the promastigote forms on transfer to promastigote growth conditions and *vice versa*. This study  
352 demonstrated that *L. orientalis* axenic amastigotes could transform to promastigote forms within 24 h and multiply in the  
353 M199 medium, pH 6.8 at 26 °C and the promastigotes that had converted back from amastigotes could also transform to  
354 amastigote form in the Grace's insect medium, pH 5.5 at 35 °C and stay in the cycle *in vitro* for at least 20 passages.

355 The *in vitro* developmental cycle of *L. orientalis* was completed within 12 days. The sequence of morphological  
356 forms of promastigotes in the cycle of *L. orientalis* resembled the forms in the natural life cycle of *L. mexicana* in a sand  
357 fly vector (*Lutzomyia longipalpis*) (Rogers et al. 2002). The complete developmental cycle was initiated with amastigotes  
358 which subsequently differentiated into procyclic forms on day 1. The procyclic population was higher on day 1-4 than  
359 other forms present, i.e., amastigotes, nectomonad promastigotes and leptomonad promastigotes, and also dividing  
360 procyclic promastigotes were observed indicating that the procyclic promastigotes multiplied in the culture. This form is  
361 responsible for the initial establishment of infection in sand flies. Then, some of them developed to be nectomonad  
362 promastigotes from day 2-7 with the highest population on day 3 and then the proportion had dropped to ~ 10% on day  
363 7. This is correlated with a biological property of nectomonad promastigotes in sand flies that this form is not a  
364 proliferative stage as reported by Rogers et al. (2002).

365 On day 3, the nectomonad promastigotes began to transform into leptomonad form. The leptomonad  
366 promastigotes dominated on day 5-7 and its proportion peaked on day 6 while the proportion of the procyclic  
367 promastigotes and the nectomonad promastigotes decreased to be less than 10% and 20%, respectively. Leptomonad  
368 promastigotes were also found in both dividing and rosette forms. The results indicated that the leptomonad form was  
369 responsible for parasite propagation. Finally, the leptomonad promastigotes differentiated into metacyclic form from day  
370 5. The highest proportion of the metacyclic promastigotes was found on day 7 at a proportion of ~ 20%. However, on day  
371 7 the proportion of the leptomonad promastigotes was ~ 43%. It is consistent with the study by Rogers et al. (2002) that  
372 leptomonad promastigotes are found ~ 30-40% after metacyclic promastigotes begin to dominate in sand flies.  
373 Leptomonad promastigotes have an important role in generation of the promastigote secretory gel (PSG). The PSG blocks  
374 the anterior parts of the sand fly midgut coincident with the accumulation of metacyclic promastigotes.

375 In addition, in this study, paramastigotes were observed from day 6 but the peak of the paramastigote population  
376 was found on day 7 at the proportion of ~ 27%. Then, the proportion fell to 3% when they were left until day 10 (data not  
377 shown). Paramastigotes could be aberrant cells, where the kinetoplast is adjacent to the nucleus (Sunter and Gull 2017).  
378 The role of paramastigotes in the sand fly vector remains unknown. In this study, no haptomonad promastigotes were  
379 found *in vitro*. Haptomonad form has been reported only in insect vectors (Rogers et al. 2002; Bates 2018). In sand flies,  
380 haptomonad promastigotes are anchored to the chitin surface of the anterior midgut by their flagella. These promastigote  
381 forms, together with the PSG, create the blocked fly that is essential for transmission (Bates 2018).

382 When the parasites on day 7 were subcultured into the medium for amastigote culture, Grace's insect medium,

383 pH 5.5 at 35 °C, the metacyclic promastigotes transformed to the amastigote-like form within 24 h and propagated until  
384 they accounted for 100% of the parasite population on day 12. This result was similar to the previous study in *L. mexicana*  
385 (Bates 1994).

386 Zymographic profiles of nucleases were used as biochemical markers to assist in defining the developmental  
387 cycle forms of *L. orientalis*. In this study, the change in morphological form of parasites was correlated with changes in  
388 the profiles of the enzymes. As discussed above, the nuclease with the apparent molecular mass of 30 kDa was found  
389 specifically in the promastigote forms of *L. orientalis*. It correlates with the results of the nucleases expressed by parasites  
390 harvested on day 4-7 in which only promastigote forms were observed. More characterization of the stage specific  
391 nuclease is required as the enzyme might be involved in different metabolisms between promastigotes and amastigotes.

392 To investigate another biological property with regard to infectivity, the ability to infect THP-1 macrophages  
393 between the axenic amastigotes and the THP-1-derived intracellular amastigotes was compared. Results revealed that  
394 both axenic amastigotes and intracellular amastigotes had the similar infection indices, average number of parasites per  
395 cell and amastigote multiplication ratio at 72 h post infection indicating that the *L. orientalis* axenic amastigotes had  
396 significant infectivity and intracellular growth *in vitro* in human macrophages.

397 In summary, the axenic cultivation of *L. orientalis* amastigotes was successfully established. The developmental  
398 cycle of *L. orientalis in vitro* was complete in 12 days using two culture systems: (1) Grace's insect medium supplemented  
399 with FCS 20%, 2% human urine, 1% BME vitamins, and 25 µg/ml gentamicin sulfate, pH 5.5 at 35 °C for amastigotes  
400 and (2) M199 medium, 10% fetal calf serum supplemented with 2% human urine, 1% BME vitamins, and 25 µg/ml  
401 gentamicin sulfate, pH 6.8 at 26 °C for promastigotes. All analyzed properties of the *L. orientalis* axenic amastigotes  
402 including morphology, biochemical properties, cyclic transformation, and infectivity to THP-1 cells were similar to the  
403 THP-1-derived intracellular amastigotes.

404 *Leishmania* parasites in the new subgenus *Mundinia* include *Leishmania enriettii*, *L. martiniquensis*, *Leishmania*  
405 *macropodum* (previously called '*Leishmania* sp. AM-2004'), and *L. orientalis* (previously called '*L. siamensis*') (Barratt  
406 et al. 2017; Jariyapan et al. 2018; Espinosa et al. 2018). Only *L. martiniquensis* and *L. orientalis* have been reported to  
407 infect humans (Jariyapan et al. 2018; Pothirat et al. 2014; Chiewchanvit et al. 2015). So far, few studies regarding *L.*  
408 *orientalis* have been conducted (Siripattanapipong et al. 2018). These authors have detected '*L. siamensis*' DNA in one  
409 female sand fly, *Sergentomyia iyengari*, however, no development of infection has been observed and transmission  
410 through the sand fly bite has not been determined. Although the proven vectors of *Leishmania* parasites are all sand flies  
411 of various species (Bates, 2007), *L. enriettii* can develop late stage infections in the biting midge *Culicoides sonorensis*  
412 and grows aggressively, producing large, ulcerated, tumor-like lesions, in guinea pigs (Seblova et al. 2015). Successful  
413 infection of *C. sonorensis* with *L. enriettii* after feeding on the ears and nose of these guinea pigs highlights that vector(s)  
414 other than sand flies should be considered on parasites belonging to the members of the subgenus *Mundinia*. Further

415 investigations of *L. orientalis*'s development in permissive vectors, such as *L. longipalpis* and *C. sonorensis*, would  
416 provide a clue for speculation on vector(s) of the parasites in nature. The availability of large quantities of uniform  
417 populations (axenic amastigotes) of *L. orientalis* would be beneficial for studies on infection and transmission  
418 mechanisms of this parasite species.

419 In conclusion, to our knowledge, this study is the first successful generation and continuous propagation of  
420 axenic amastigotes of *L. orientalis*. Also, its complete developmental sequence in the axenic culture was described. Both  
421 *in vitro* culture systems would provide a useful tool for the generation of large amounts of pure and viable parasite  
422 populations of each stages or forms for further studies on cell and molecular biology, biochemistry, and others, especially,  
423 mechanisms involved in infection, survival and development in permissive vector(s) and host(s). These results would be  
424 useful and invaluable in increasing the understanding of *L. orientalis* biology and for developing strategies to control and  
425 eliminate *Leishmania* parasites.

426

#### 427 **Acknowledgements**

428 We thank Assoc. Prof. Dr. Sirida Yangshim of the Department of Microbiology, Faculty of Medicine, Chiang Mai  
429 University for the human monocytic cell line.

430

#### 431 **Funding**

432 This work was supported by the Thailand Research Fund through the Royal Golden Jubilee Ph.D. Program (grant  
433 number: PHD/0065/2556 to NJ for WC), the Faculty of Medicine Endowment Fund (grant number: 024/2558 to NJ),  
434 and the Diamond Research Grant (grant number: PAR-2560-04663 to NJ), Faculty of Medicine, Chiang Mai  
435 University. In addition we acknowledge the Chiang Mai University for providing the budget for our Excellence Center  
436 in Insect Vector Study (grant number: 2562 to NJ). The funders had no role in study design, data collection and  
437 analysis, decision to publish, or preparation of the manuscript.

438

#### 439 **Compliance with ethical standards**

440

#### 441 **Conflict of interests**

442 The authors declare that they have no conflict of interests.

443

#### 444 **Author contributions**

445 NJ and PAB conceived and designed study. WC and MDB performed research. NJ, PS, and WC analyzed data. NJ, WC  
446 and PAB wrote the paper. All authors read and approved the final version of the manuscript.

447

448 **References**

- 449 Akhoundi M, Downing T, Votýpka J et al (2017) *Leishmania* infections: Molecular targets and diagnosis. *Mol Aspects*  
450 *Med* 57:1-29
- 451 al-Bashir NT, Rassam MB, al-Rawi BM (1992) Axenic cultivation of amastigotes of *Leishmania donovani* and  
452 *Leishmania major* and their infectivity. *Ann Trop Med Parasitol* 86:487-502
- 453 Barratt J, Kaufer A, Peters B, et al (2017) Isolation of novel Trypanosomatid, *Zelonia australiensis* sp. nov.  
454 (Kinetoplastida:Trypanosomatidae) provides support for a Gondwanan origin of dixenous parasitism in the  
455 Leishmaniinae. *PLoS Negl Trop Dis* 11:e0005215
- 456 Bates PA (1994) Complete developmental cycle of *Leishmania mexicana* in axenic culture. *Parasitology* 108:1-9
- 457 Bates PA (2007) Transmission of *Leishmania* metacyclic promastigotes by phlebotomine sand flies. *Int J Parasitol*  
458 37:1097-1106
- 459 Bates PA (2018) Revising *Leishmania's* life cycle. *Nat Microbiol* 3:529-530
- 460 Bates PA, Robertson CD, Tetley L et al (1992) Axenic cultivation and characterization of *Leishmania mexicana*  
461 amastigote-like forms. *Parasitology* 105:193-202
- 462 Chiewchanvit S, Tovanabutra N, Jariyapan N et al (2015) Chronic generalized fibrotic skin lesions from disseminated  
463 leishmaniasis caused by *Leishmania martiniquensis* in two patients from northern Thailand infected with HIV.  
464 *Br J Dermatol* 173:663-670
- 465 Debrabant A, Joshi MB, Pimenta PF et al (2004) Generation of *Leishmania donovani* axenic amastigotes: their growth  
466 and biological characteristics. *Int J Parasitol* 34:205-217
- 467 Espinosa OA, Serrano MG, Camargo EP et al (2018) An appraisal of the taxonomy and nomenclature of  
468 trypanosomatids presently classified as *Leishmania* and *Endotrypanum*. *Parasitology* 145:430-442
- 469 Ghosh S, Goswami S, Adhya S (2003) Role of superoxide dismutase in survival of *Leishmania* within the macrophage.  
470 *Biochem J* 369:447-452
- 471 Gupta N, Goyal N, Rastogi AK (2001) *In vitro* cultivation and characterization of axenic amastigotes of *Leishmania*.  
472 *Trends Parasitol* 17:150-153
- 473 Hodgkinson VH, Soong L, Duboise SM et al (1996) *Leishmania amazonensis*: cultivation and characterization of  
474 axenic amastigote-like organisms. *Exp Parasitol* 83:94-105
- 475 Jain SK, Sahu R, Walker LA et al (2012) A parasite rescue and transformation assay for antileishmanial screening  
476 against intracellular *Leishmania donovani* amastigotes in THP1 human acute monocytic leukemia cell line. *J*  
477 *Vis Exp* 70:4054
- 478 Jariyapan N, Daroontum T, Jaiwong K et al (2018) *Leishmania (Mundinia) orientalis* n. sp. (Trypanosomatidae), a

479 parasite from Thailand responsible for localized cutaneous leishmaniasis. *Parasit Vectors* 11:351

480 Joshi MB, Hernandez Y, Owings JP et al (2012) Diverse viscerotropic isolates of *Leishmania* all express a highly

481 conserved secretory nuclease during human infections. *Mol Cell Biochem* 361:169-179

482 Li J, Zheng ZW, Natarajan G et al (2017) The first successful report of the in vitro life cycle of Chinese *Leishmania*: the

483 in vitro conversion of *Leishmania* amastigotes has been raised to 94% by testing 216 culture medium

484 compound. *Acta Parasitol* 62:154-163

485 Moradin N, Descoteaux A (2012) *Leishmania* promastigotes: building a safe niche within macrophages. *Front Cell*

486 *Infect Microbiol* 2:121

487 Paladi Cde S, Pimentel IA, Katz S et al (2012) *In vitro* and *in vivo* activity of a palladacycle complex on *Leishmania*

488 (*Leishmania*) *amazonensis*. *PLoS Negl Trop Dis* 6:e1626

489 Pan AA (1984) *Leishmania mexicana*: serial cultivation of intracellular stages in a cell-free medium. *Exp Parasitol*

490 58:72-80

491 Pothirat T, Tantiworawit A, Chaiwarith R et al (2014) First isolation of *Leishmania* from Northern Thailand: case

492 report, identification as *Leishmania martiniquensis* and phylogenetic position within the *Leishmania enriettii*

493 complex. *PLoS Negl Trop Dis* 8:e3339

494 Rainey PM, Spithill TW, McMahon-Pratt D et al (1991) Biochemical and molecular characterization of *Leishmania*

495 *pifanoi* amastigotes in continuous axenic culture. *Mol Biochem Parasitol* 49:111-118

496 Rogers ME, Chance ML, Bates PA (2002) The role of promastigote secretory gel in the origin and transmission of the

497 infective stage of *Leishmania mexicana* by the sandfly *Lutzomyia longipalpis*. *Parasitology* 124:495-507

498 Saar Y, Ransford A, Waldman E et al (1998) Characterization of developmentally-regulated activities in axenic

499 amastigotes of *Leishmania donovani*. *Mol Biochem Parasitol* 95:9-20

500 Seblova V, Sadlova J, Vojtkova B et al (2015) The biting midge *Culicoides sonorensis* (Diptera: Ceratopogonidae) is

501 capable of developing late stage infections of *Leishmania enriettii*. *PLoS Negl Trop Dis* 9:e0004060

502 Späth GF, Beverley SM (2001) A lipophosphoglycan-independent method for isolation of infective *Leishmania*

503 metacyclic promastigotes by density gradient centrifugation. *Exp Parasitol* 99:97-103

504 Schuster FL, Sullivan JJ (2002) Cultivation of clinically significant hemoflagellates. *Clin Microbiol Rev* 15:374-389

505 Siripattanapipong S, Leelayoova S, Ninsaeng U et al (2018) Detection of DNA of *Leishmania siamensis* in

506 *Sergentomyia* (*Neophlebotomus*) *iyengari* (Diptera: Psychodidae) and molecular identification of blood meals

507 of sand flies in an affected area, Southern Thailand. *J Med Entomol* 55:1277-1283

508 Sunter J, Gull K (2017) Shape, form, function and *Leishmania* pathogenicity: from textbook descriptions to biological

509 understanding. *Open Biol* 7:170165

510 Teixeira MC, de Jesus Santos R, Sampaio RB et al (2002) A simple and reproducible method to obtain large numbers of



511 axenic amastigotes of different *Leishmania* species. Parasitol Res 88:963-968

512 Yao C, Chen Y, Sudan B et al (2008) *Leishmania chagasi*: homogenous metacyclic promastigotes isolated by buoyant  
513 density are highly virulent in a mouse model. Exp Parasitol 118:129-133

514

515 **Table 1** Percent purity of parasite forms of *L. orientalis* expressed as mean  $\pm$  standard deviation

| Form                                 | Days of collection |                  |                  |                  |                  |
|--------------------------------------|--------------------|------------------|------------------|------------------|------------------|
|                                      | 0 <sup>a</sup>     | 2 <sup>b</sup>   | 3 <sup>b</sup>   | 5 <sup>c</sup>   | 7 <sup>c</sup>   |
| Intracellular amastigote             | 100                | 10.33 $\pm$ 1.53 | 0.33 $\pm$ 0.58  | 0                | 0                |
| Procyclic promastigote               | 0                  | 89.67 $\pm$ 1.53 | 7.33 $\pm$ 0.58  | 0                | 0                |
| Nectomonad promastigote <sup>d</sup> | 0                  | 0                | 85.67 $\pm$ 1.53 | 3.67 $\pm$ 1.53  | 9.00 $\pm$ 2.00  |
| Leptomonad promastigote <sup>d</sup> | 0                  | 0                | 6.67 $\pm$ 0.58  | 88.00 $\pm$ 1.73 | 6.33 $\pm$ 1.15  |
| Metacyclic promastigote <sup>d</sup> | 0                  | 0                | 0                | 8.33 $\pm$ 2.52  | 84.67 $\pm$ 3.06 |

516 <sup>a</sup>Pure intracellular amastigotes harvested from infected THP-1 macrophages

517 <sup>b</sup>Day of collection from passage 0

518 <sup>c</sup>Day of collection from passage 1

519 <sup>d</sup>Parasitic form enriched by discontinuous Ficoll gradient centrifugation

520

521 **Table 2** Morphological categories of *L. orientalis*

| Morphological category <sup>a</sup> | Criteria   |
|-------------------------------------|--|
| Amastigote                          | Oval body form, no flagellum protruding from flagellar pocket                      |
| Procyclic promastigote              | Body length 8-11.5 $\mu$ m flagellum < body length                                 |
| Nectomonad promastigote             | Body length $\geq$ 12.5 $\mu$ m, body width and flagellum length varied            |
| Leptomonad promastigote             | Body length 8.0-11.5 $\mu$ m flagellum $\geq$ body length                          |
| Metacyclic promastigote             | Body length < 12.5 $\mu$ m, body width $\leq$ 1.5 $\mu$ m, flagellum > body length |
| Paramastigote                       | Kinetoplast adjacent to nucleus, external flagellum present                        |

522 <sup>a</sup>Based on descriptions by (Rogers et al. 2002)

523

524 **Table 3** Morphological features of *L. orientalis* including cell body length and width, flagellum length, and nuclear-

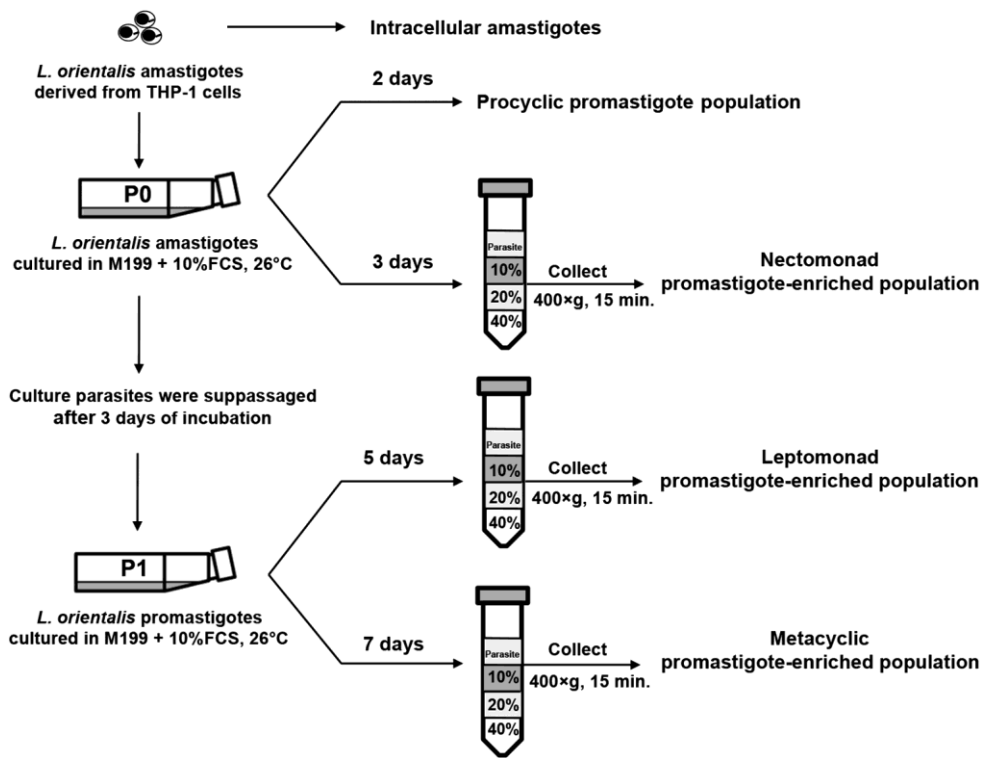
525 kinetoplast position measured and expressed as mean  $\pm$  standard deviation

| Morphological category  | Morphological feature  |                       |                             |                                 |                             |
|-------------------------|------------------------|-----------------------|-----------------------------|---------------------------------|-----------------------------|
|                         | Body length ( $\mu$ m) | Body width ( $\mu$ m) | Flagellum length ( $\mu$ m) | Anterior-kinetoplast ( $\mu$ m) | Anterior-nucleus ( $\mu$ m) |
| Amastigote              | 4.90 $\pm$ 0.45        | 2.34 $\pm$ 0.33       | -                           | -                               | -                           |
| Procyclic promastigote  | 9.33 $\pm$ 1.45        | 2.23 $\pm$ 0.35       | 7.55 $\pm$ 2.19             | 2.28 $\pm$ 0.66                 | 4.24 $\pm$ 0.67             |
| Nectomonad promastigote | 15.10 $\pm$ 2.07       | 2.15 $\pm$ 0.30       | 19.65 $\pm$ 3.95            | 2.60 $\pm$ 0.70                 | 5.41 $\pm$ 0.79             |
| Leptomonad promastigote | 10.68 $\pm$ 1.00       | 2.35 $\pm$ 0.32       | 15.20 $\pm$ 3.42            | 2.24 $\pm$ 0.32                 | 4.39 $\pm$ 0.54             |
| Metacyclic promastigote | 10.04 $\pm$ 1.59       | 1.11 $\pm$ 0.22       | 16.93 $\pm$ 2.54            | 2.15 $\pm$ 0.52                 | 4.22 $\pm$ 0.76             |
| Paramastigote           | 8.43 $\pm$ 1.58        | 2.89 $\pm$ 0.40       | 14.63 $\pm$ 3.13            | 2.97 $\pm$ 0.73                 | 3.43 $\pm$ 0.70             |

526

527 **Figure captions**

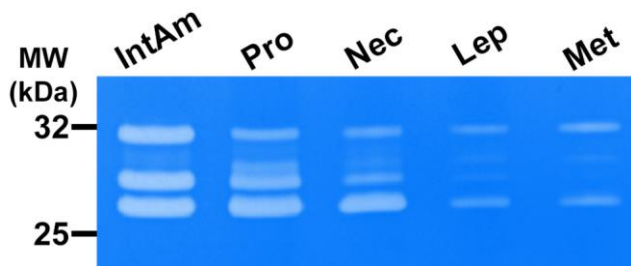
528



529

530 **Fig. 1** Schematic illustration for enrichment of *L. orientalis* nectomonad promastigotes, leptomonad promastigotes, and  
531 metacyclic promastigotes using discontinuous Ficoll gradient centrifugation and collection of samples for zymographic  
532 analysis of nucleases

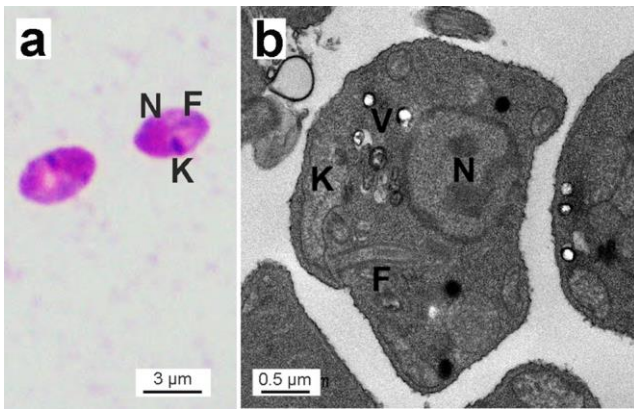
533



534

535 **Fig. 2** Zymographic profiles of nucleases of THP-1 derived intracellular amastigotes (IntAm), procyclic promastigote-  
536 enriched population (Pro), nectomonad promastigote-enriched population (Nec), leptomonad promastigote-enriched  
537 population (Lep), and metacyclic promastigote-enriched population (Met)

538

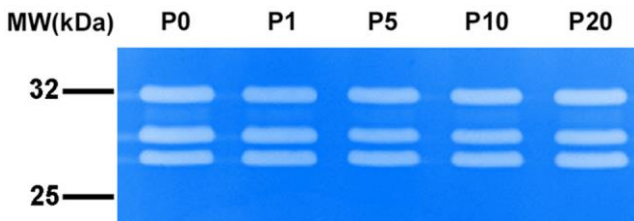


539

540 **Fig. 3** *L. orientalis* axenic amastigotes showing kinetoplast (K), nucleus (N), flagellum (F), and vacuole (V). **a** LM. **b**

541 TEM

542

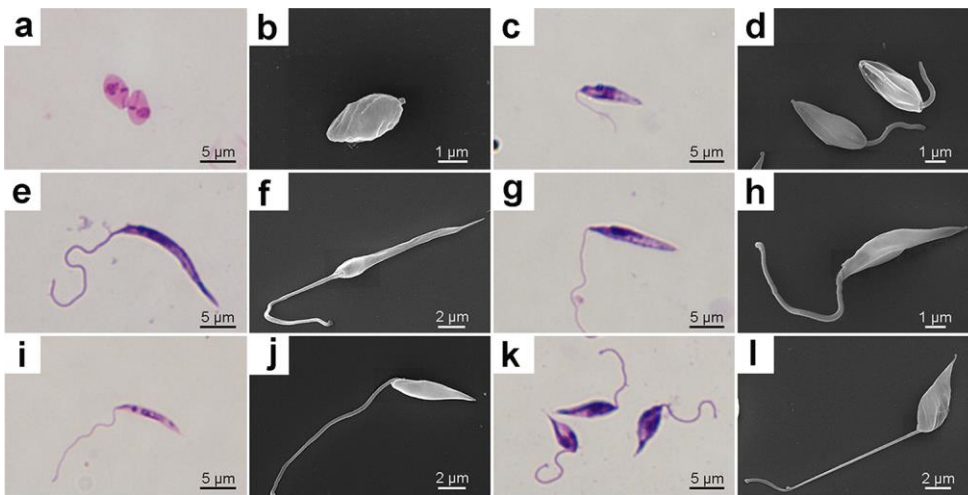


543

544 **Fig. 4** Zymographic profiles of nucleases of axenic amastigotes from different parasite subpassages (P0, P1, P5, P10, and

545 P20)

546



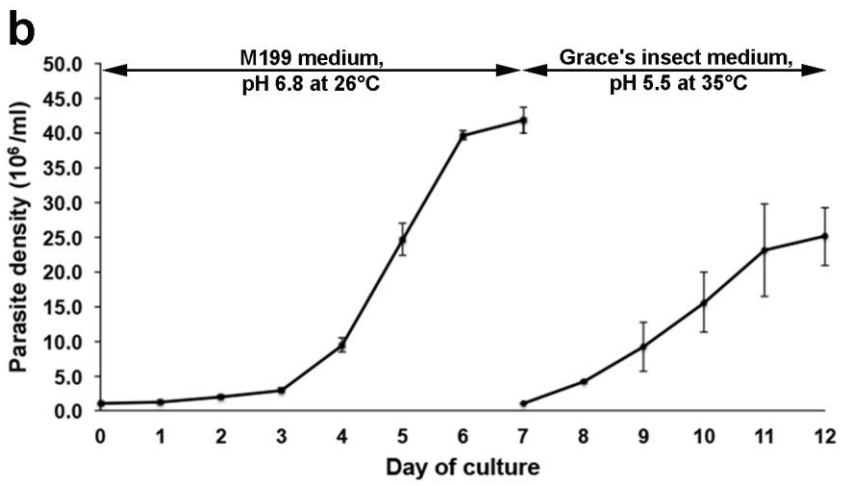
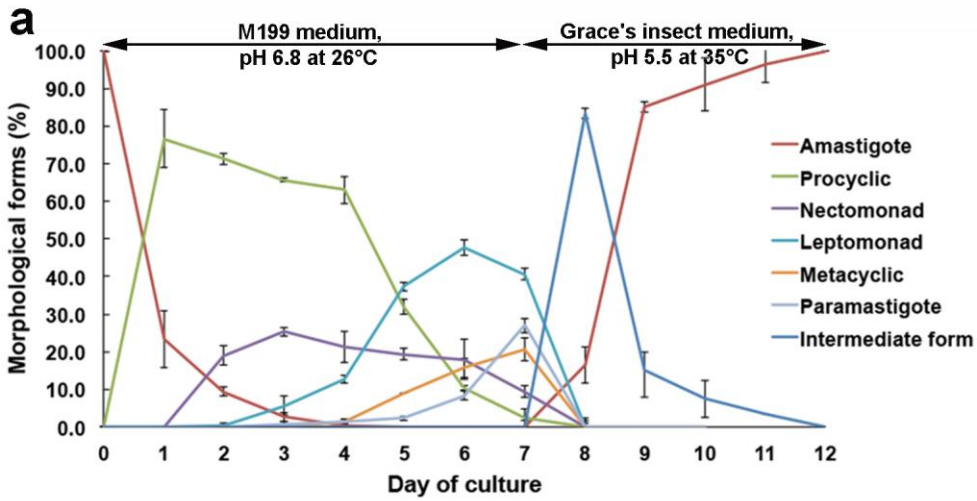
547

548 **Fig. 5** Six developmental forms of *L. orientalis* in the axenic culture including amastigotes (**a, b**); procyclic promastigotes

549 (**c, d**); nectomonad promastigotes (**e, f**); leptomonad promastigotes (**g, h**); metacyclic promastigotes (**i, j**); and

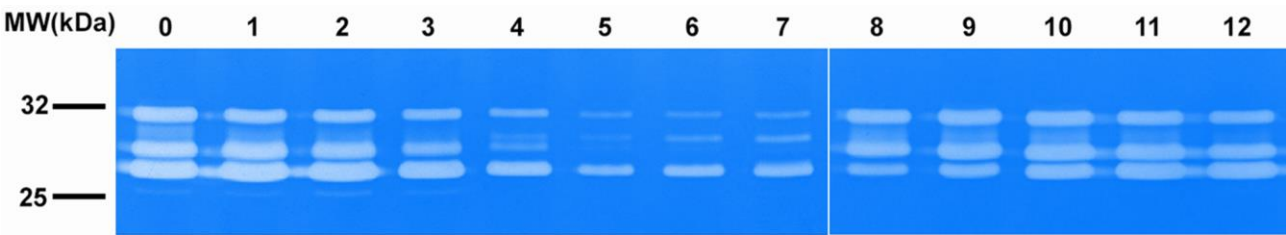
550 paramastigotes (**k, l**). LM micrographs = **a, c, e, g, i, and k**. SEM micrographs = **b, d, f, h, j, and l**

551



552

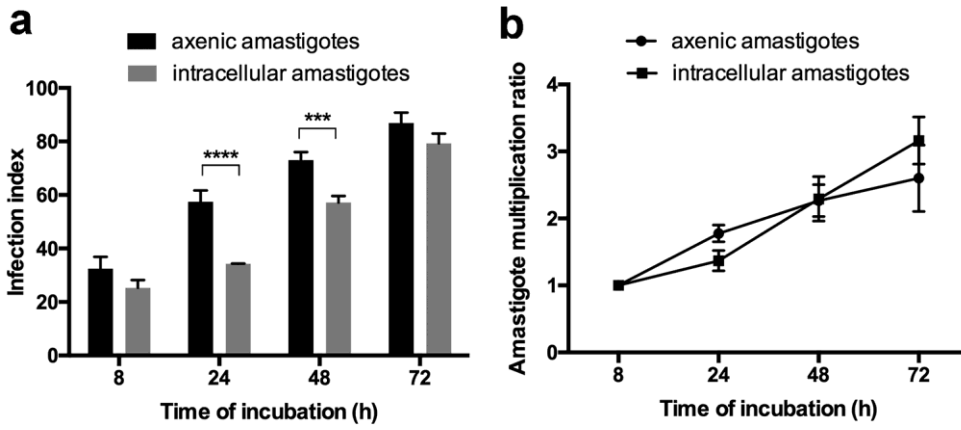
553 **Fig. 6** Sequential development of *L. orientalis* parasites in the culture. **a** Morphological forms present on day 1-12 **b** Parasite  
554 density in the cultures from day 1-12



555

556 **Fig. 7** Nuclease zymographic profiles of parasite lysates from cells harvested throughout the development in axenic  
557 culture (day 0-12). Noted that on day 0-7 the parasites were in the M199 medium and on day 8-12 the parasites were in  
558 the Grace's insect medium

559



560

561

562

563

564

**Fig. 8 a** Infection index of *L. orientalis* axenic and THP-1-derived intracellular amastigotes to THP-1 cells at different time points. Results are expressed as mean  $\pm$  standard deviation and based on three independent replicates. \*\*\*P < 0.001; \*\*\*\*P < 0.0001. **b** Amastigote multiplication ratio of *L. orientalis* axenic and intracellular amastigotes in THP-1 cells. Results are expressed as mean  $\pm$  standard deviation and based on three independent replicates